

# La enhances IRES-mediated translation of laminin B1 during malignant epithelial to mesenchymal transition

Michaela Petz<sup>1</sup>, Nicole Them<sup>1</sup>, Heidemarie Huber<sup>1</sup>, Hartmut Beug<sup>2,†</sup> and Wolfgang Mikulits<sup>1,\*</sup>

<sup>1</sup>Department of Medicine I, Division: Institute of Cancer Research, Comprehensive Cancer Center Vienna, Medical University of Vienna, Borschkegasse 8a, 1090 Vienna and <sup>2</sup>Institute for Animal Breeding and Genetics, University of Veterinary Medicine I, Veterinärplatz 1, 1210 Vienna, Austria

Received March 9, 2011; Revised July 26, 2011; Accepted August 21, 2011

## ABSTRACT

The majority of transcripts that harbor an internal ribosome entry site (IRES) are involved in cancer development via corresponding proteins. A crucial event in tumor progression referred to as epithelial to mesenchymal transition (EMT) allows carcinoma cells to acquire invasive properties. The translational activation of the extracellular matrix component laminin B1 (LamB1) during EMT has been recently reported suggesting an IRES-mediated mechanism. In this study, the IRES activity of LamB1 was determined by independent bicistronic reporter assays. Strong evidences exclude an impact of cryptic promoter or splice sites on IRES-driven translation of LamB1. Furthermore, no other LamB1 mRNA species arising from alternative transcription start sites or polyadenylation signals were detected that account for its translational control. Mapping of the LamB1 5'-untranslated region (UTR) revealed the minimal LamB1 IRES motif between –293 and –1 upstream of the start codon. Notably, RNA affinity purification showed that the La protein interacts with the LamB1 IRES. This interaction and its regulation during EMT were confirmed by ribonucleoprotein immunoprecipitation. In addition, La was able to positively modulate LamB1 IRES translation. In summary, these data indicate that the LamB1 IRES is activated by binding to La which leads to translational upregulation during hepatocellular EMT.

## INTRODUCTION

The interaction of tumor cells with the extracellular matrix (ECM) is essential for cancer invasion and metastasis.

Laminins constitute the ECM as the main non-collagenous glycoproteins of the basement membrane and affect the migratory behavior of a variety of malignant cell types (1). Laminin B1 (LamB1) represents one moiety of the three  $\beta$ -subunits that assemble with  $\alpha$ - and  $\gamma$ -chains to form a multitude of heterotrimeric laminin isoforms (2). LamB1 modulates laminin-mediated integrin signaling that promotes cell adhesion, motility and differentiation (3). In addition, LamB1 is the ligand of the monomeric 67-kDa laminin receptor [LamR; (4–6)] that drives tumor cell invasion as well as angiogenesis and is strongly expressed in many metastatic cancers (7–9). The overexpression of LamB1 has been particularly reported in hepatocellular carcinoma (HCC), which is frequently preceded by fibrosis and cirrhosis and thus accompanied by increased ECM deposition. Accordingly, LamB1 expression is augmented during transforming growth factor (TGF)- $\beta$  induced liver fibrosis of transgenic mice (10). Proteome analysis of HCC patients revealed a rise of LamB1 levels in cirrhotic tissue and a further increase in carcinoma cells (11). The elevated LamB1 expression in HCC associates with upregulation of  $\beta$ 1 integrin and LamR (12–14).

A crucial event in tumor progression is the gain of invasive properties of carcinoma cells by epithelial to mesenchymal transition (EMT). This process is characterized by the loss of epithelial cell polarity and acquisition of a fibroblastoid phenotype enabling tumor cells to leave epithelial cell organization (15). In HCC cells, EMT can be induced by the synergy of TGF- $\beta$  and oncogenic Ras signaling, which are frequently activated in HCC patients (15–18). Recently, we showed that LamB1 is translationally upregulated in HCC cells that have undergone EMT through the cooperation of TGF- $\beta$  with Ras (19). The translational activation of LamB1 was proposed to be regulated by an internal ribosome entry site (IRES).

\*To whom correspondence should be addressed. Tel: +43 1 4277 65250; Fax: +43 1 4277 65239; Email: wolfgang.mikulits@meduniwien.ac.at

†Deceased.

The IRES secondary structure located within the 5'-untranslated region (UTR) of the mRNA allows direct ribosome binding and translation initiation independently of the cap structure. Translation of key regulatory proteins that are involved in cancer-relevant processes such as angiogenesis, mitosis and apoptosis is frequently driven by internal initiation (20). IRES-translated transcripts escape from downregulation of cap-dependent protein synthesis and foster tumor cells to overcome stress conditions induced by hypoxia or nutrient deprivation (21). Deregulation of translation control affects IRES-mediated translation in a dual way. Cap-dependent translation of IRES-competent transcripts is increased in the presence of high levels of activated translation initiation factor eIF4E, while same transcripts are translated by IRES-dependent mechanism when eIF4E is downregulated in response to cellular stress or other stimuli (22,23). Furthermore, IRES-mediated translation is regulated by IRES transacting factors (ITAFs) which mainly comprise heterogeneous nuclear ribonucleoproteins (hnRNPs) that shuttle between cytoplasm and nucleus (24). ITAFs selectively bind IRES structures and modulate their activity, allowing a distinguished response of IRES transcripts to cellular conditions that affect translation. A role of ITAFs in regulating cell survival and angiogenesis has been described although little is known about tumor-associated alterations of ITAFs (25).

Here we demonstrate that the 5'-UTR of LamB1 harbors a *bona fide* IRES structure localized between -293 and -1 upstream of the start codon. RNA affinity purification as well as *in vivo* UV crosslinking combined with RNP immunoprecipitation allowed the identification of La protein as an ITAF that binds to the LamB1 IRES. Moreover, La was found to positively regulate the LamB1 IRES activity which might account for the increased IRES mediated LamB1 translation of EMT-transformed hepatocytes.

## MATERIAL AND METHODS

### Construction of the plasmids

The LamB1 5'-UTR was cloned downstream of the Firefly luciferase open reading frame (ORF) into p-F resulting in pLam-F(19). Primers were designed according to GenBank sequence NM\_002291. Plasmids for the cryptic promoter assay were generated by removal of the CMV promoter from pF, pLam-F and pEMCV-F (19). Bicistronic plasmids were constructed based on the pβgal/5'(-162)/CAT vector (a kind gift from Dr Martin Holcik) (26). The XIAP IRES sequence was removed from pβgal/5'(-162)/CAT to generate the empty control vector pβgal/CAT, or replaced by the LamB1 5'-UTR resulting in pβgal/Lam/CAT. Deletion fragments for the mapping of the 5'-UTR were amplified by PCR and cloned into pβgal/CAT. Primer sequences are shown in [Supplementary Table S1](#). Plasmids for the streptavidin-tethered RNA affinity purification were generated by inserting the LamB1 5'-UTR or the minimal XIAP IRES sequence into the pTrap vector (kindly provided by

Dr Martin Dienstbier) (27). Primer sequences are shown in [Supplementary Table S2](#).

### Cell culture

Immortalized murine MIM-1-4 hepatocytes were grown on collagen-coated culture dishes in RPMI 1640 plus 10% fetal calf serum (FCS), 40 ng/ml human TGF- $\alpha$  (Sigma, St. Louis, USA), 30 ng/ml human insulin-like growth factor II (IGF-II, Sigma, St. Louis, USA), 1.4 nM insulin (Sigma, St. Louis, USA) and antibiotics, as described previously (28). Malignant epithelial MIM-R hepatocytes are derived from MIM-1-4 cells by expressing oncogenic Ha-Ras and green fluorescent protein as outlined recently (29). TGF- $\beta$ 1 (R&D Systems, Minneapolis, USA) was used at a concentration of 2.5 ng/ml for the first 72 h of EMT induction. For long-term treatment of MIM-R hepatocytes, TGF- $\beta$ 1 was supplemented to the medium at a concentration of 1 ng/ml, resulting in fibroblastoid MIM-RT cells after >2 weeks. Human SW480 and HEK293 cells were cultured in DMEM and HepG2 cells in MNP each plus 10% FCS. The human HCC cell lines Hep3B and AKH3p were grown in RPMI 1640 medium supplemented with 10% FCS. All cells were kept at 37°C and 5% CO<sub>2</sub> and routinely screened for the absence of mycoplasma.

### Western blot analysis

The preparation of cellular extracts, separation of proteins by SDS-PAGE and immunoblotting were performed as described recently (18). Cytoplasmic and nuclear cell fractions were generated using a Proteo-JET<sup>®</sup> kit (Fermentas, St. Leon-Rot, Germany) according to the manufacturers' description. A total of 30  $\mu$ g protein extract was loaded onto gels and immunological detection of proteins was performed with the Super Signal detection system (Pierce Chemical Company, Rockford, USA). The following primary antibodies were used: anti-laminin B1 (Neo Markers, Fremont, USA), 1:1000; anti-hnRNP A1 (Santa Cruz Biotechnology, California, USA), 1:1000; anti-actin (Sigma, St. Louis, USA), 1:2000; anti-La (Santa Cruz Biotechnology, California, USA) and (Cell Signaling, MA, USA), 1:1000; anti-tubulin (Sigma, St. Louis, USA), 1:1000; anti-nucleoporin (BD Biosciences, NJ, USA), 1:1000. Secondary antibodies (Calbiochem, La Jolla, USA) were used at dilutions of 1:10 000.

### Reverse transcriptase (RT)-polymerase chain reaction (PCR), quantitative (q)PCR and RACE-PCR

RNA was extracted, DNaseI treated and reverse transcribed using a RNA isolation and cDNA synthesis kit (Quiagen, Hilden, Germany) as recommended by the manufacturer. Aliquots of the cDNA were employed for Reverse transcriptase-polymerase chain reaction (RT-PCR) using Ready-To-Go PCR beads (Amersham, Uppsala, Sweden). Amplification products of semi-quantitative PCR were visualized by ethidium bromide staining on a 1% agarose gel. Primer sequences are shown in [Supplementary Table S3](#). qPCR was performed with Fast SYBR green (Applied Biosystems, CA, USA) according to the recommendations of the manufacturer

and quantified with the 7500 Fast Real Time PCR System (Applied Biosystems). Primer sequences are shown in [Supplementary Table S4](#). 5'- and 3'-RACE-PCR was performed using a First Choice® RLM-RACE Kit (Applied Biosystems, CA, USA) according to the manufacturer's recommendation. Primer sequences are shown in [Supplementary Table S5](#).

### Transient transfection and reporter assays

Cells were plated on six-well plates and transiently transfected after 24 h with Lipofectamine Plus as recommended by the manufacturer (Invitrogen, Carlsbad, USA). Cells were lysed 48 h post-transfection and enzymatic reporter activities were determined. Luciferase activity was measured with a Luminoskan microplate reader (Labsystems, Farnborough, UK) as recently described (19).  $\beta$ -galactosidase ( $\beta$ -gal) activity was photometrically determined using *o*-nitrophenyl- $\beta$ -D-galactopyranoside and chloramphenicol acetyltransferase (CAT) activity was measured by ELISA (Roche, Mannheim, Germany) as recommended by the manufacturer. In assays analyzing the interference of cap-dependent translation, reporter activities were normalized to mRNA levels as quantified by qPCR. Otherwise, relative IRES activity of bicistronic assays was calculated as the ratio of CAT/ $\beta$ -gal. Luciferase activities of monocistronic vectors were normalized to  $\beta$ -gal activities of a co-transfected  $\beta$ -gal reporter (19). Assays were performed in triplicate and results represent the average of three independent experiments.

### RNA-protein immunoprecipitation

Cells were transfected with a bicistronic vector as described above or directly UV crosslinked with 400 mJ/cm<sup>2</sup> before cell lysis. Lysates were centrifuged at 1200g and supernatants were aliquoted corresponding to  $3 \times 10^6$  cells. An amount of 5  $\mu$ g La antibody (Santa Cruz Biotechnology, California, USA) were crosslinked to 50  $\mu$ l Dynabeads® Protein A (Invitrogen, California, USA) using Bis(sulfosuccinimidyl)suberate (BS<sup>3</sup>; Thermo Fisher Scientific, Massachusetts, USA) as described by the manufacturer. Crosslinked Dynabeads® were incubated with aliquots of pre-cleared cell lysates at room temperature, washed and the immunoprecipitated RNA-protein complexes were eluted at 95°C. Eluates were treated with proteinase K (Fermentas, St. Leon-Rot, Germany) and the RNA was ethanol-precipitated after extraction with phenol-chloroform. After treatment with DNaseI (Fermentas), mRNA was purified using a mRNA isolation kit (Roche, Mannheim, Germany) and subjected to cDNA synthesis. Subsequent RT-PCR or qPCR was performed as described above. To determine the amount of input RNA that was used for immunoprecipitation, RNA was isolated from aliquots of cell lysates using a RNA isolation kit (Quiagen, Hilden, Germany), treated with proteinase K and processed as described above. The buffer for cell lysis and immunoprecipitation consisted of 30 mM HEPES pH 7.3, 160 mM KCl, 2.5 mM MgCl<sub>2</sub>, 1 mM DTT, 0.1% NP-40, 0.5% Triton X-100 and 10% glycerol. The washing buffer included PBS pH 7.4 and 0.02% Tween. The elution buffer was composed of

100 mM Tris-HCl pH 7.4, 5% SDS, 70 mM  $\beta$ -mercaptoethanol and 5 mM DTT.

### Northern blot analysis

Cells were grown on a 6-cm culture dish and transfected with bicistronic vectors using Lipofectamine Plus as recommended by the manufacturer (Invitrogen, Carlsbad, USA). mRNA was isolated with a mRNA isolation kit (Roche, Mannheim, Germany). RNA samples were heated at 65°C for 15 min in RNA sample buffer, cooled on ice and separated on a MOPS-formaldehyde agarose gel. RNA was transferred to a membrane (NEN life science products, MA, USA) and UV crosslinked. Probes were amplified by PCR from the p $\beta$ gal/Lam/CAT vector in the presence of <sup>32</sup>P-labeled dCTP. Primer sequences are described in [Supplementary Table S6](#). Unincorporated nucleotides were removed using a Gel extraction Kit (Quiagen, Hilden, Germany). Membranes were pre-hybridized for 4 h and then hybridized over night at 42°C with  $5 \times 10^7$  cpm of radiolabeled probe. Membranes were washed at 65°C and exposed to x-ray films at -80°C.

### In vitro translation

Bicistronic vectors containing the Lamb1 5'-UTR or XIAP IRES were *in vitro* transcribed using a MEGAscript® kit (Applied Biosystems, CA, USA). Rabbit reticulocyte lysate (RRL) (Promega, Madison, USA) was programmed with the transcripts and *in vitro* translation was performed according to the guidelines of the manufacturer. CAT activities were determined by ELISA (Roche, Mannheim, Germany) and normalized to transcript levels quantified by CAT RT-PCR. In order to pre-clear the reticulocyte lysate from La, 5  $\mu$ g La antibody was crosslinked to 50  $\mu$ l Dynabeads® Protein A (Invitrogen, California, USA) by using BS<sup>3</sup> as described by the manufacturer (Thermo Fisher Scientific, Massachusetts, USA). Reticulocyte lysate was incubated with crosslinked Dynabeads® for 30 min at room temperature followed by removal of Dynabeads®. An amount of 1  $\mu$ g of recombinant La (Prospec, Rehovot, Israel) was added to reconstitute La activity. Results show the average of three independent experiments.

### Streptavidin-tethered RNA affinity purification

A total of  $2 \times 10^7$  cells were lysed and pre-cleared with 50  $\mu$ l streptavidin-linked magnetic beads (Sigma, St. Louis, USA). Another 50  $\mu$ l of magnetic beads were washed and resuspended in 200  $\mu$ l buffer. An amount of 5  $\mu$ g of *in vitro* transcribed S1-aptamer fused RNA and 5  $\mu$ l RNasin (Promega, Madison, USA) were added and the beads were incubated on a thermomixer for 90 min at 4°C with moderate shaking. RNA-associated beads were washed with 200  $\mu$ l buffer and further incubated with the pre-cleared protein extract on a thermomixer for 90 min at 4°C while shaking. Beads were then washed five times with buffer. RNA-protein complexes were eluted by incubating with buffer containing biotin at a final concentration of 10 mM at 4°C for 160 min. Eluted proteins were analyzed by SDS-PAGE followed by silver staining or western blot. The buffer used for cell lysis, affinity chromatography,



washing and elution contained 30 mM HEPES, pH 7.3, 160 mM KCl, 2.5 mM MgCl<sub>2</sub>, 1 mM DTT, 0.1% NP-40, 0.5% Triton X-100 and 10% glycerol.

Stable knock-down of La

MISSION<sup>®</sup> shRNA lentiviral transduction particles (Sigma, St. Louis, USA) were used to knock-down La (NM\_009278) in MIM-R and MIM-RT hepatocytes. Cells were transduced with viral particles containing shRNA against La (TRCN0000071284, TRCN0000071287) or non-target shRNA (SHC002V) in a pLKO.1 vector and treated with puromycin (5 µg/ml) for selection.

Statistical analysis

Data were expressed as means ± SD. The statistical significance of differences was evaluated using a paired, non-parametric Student's *t*-test. Significant differences between experimental groups were \**P* < 0.05, \*\**P* < 0.01 or \*\*\**P* < 0.005.

RESULTS

LamB1 mRNA in cancer cells

Recently we identified the cap-independent translational upregulation of LamB1 during TGF-β-induced EMT of epithelial MIM-R hepatocytes to invasive, fibroblastoid MIM-RT cells (19). To further assess translational control of LamB1 during EMT, we studied a conceivable impact of LamB1 mRNA isoforms. Differential utilization of transcripts generated by e.g. alternative splicing is known to cause aberrant gene expression during oncogenesis (30). Notably, the LamB1 5'-UTR sequence published in NCBI (NM\_002291.2) is not entirely supported by expressed sequence tags (ESTs) or full length cDNA.

Rather, the EST database dbEST contains transcripts that start at -147 nt or further downstream and fail to confirm the region from -335 to -154 in the 5'-UTR. *In silico* analysis of the 5'-UTR using Zuckers mfold version 4.11 predicted a strong secondary structure with a minimal free energy of -154 kcal/mol which could account for insufficient amplification and could explain missing ESTs (31,32). Therefore, we tested whether the first 1-181 nt of the published sequence were amplified from DNA contaminations. Interestingly, RT-PCR analysis of different human cell lines after DNase treatment showed amplification of the entire 5'-UTR sequence comprising 335 nt as published in NCBI (Figure 1A). Combined DNase and RNase treatment failed to show amplicons, excluding the presence of DNA. Thus, our data confirm the expression of the published human LamB1 5'-UTR sequence.

Furthermore, we performed RACE-PCR of the 5'- and 3'-UTR to identify any transcript variants that may be involved in translational regulation of LamB1 (Figure 1B). In accordance, we were able to amplify a single 335-nt long 5'-UTR sequence in various human cancer cell lines. No other transcripts were detected suggesting the absence of alternative splice products of the LamB1 5'-UTR. In addition, we analyzed variations in the LamB1 3'-UTR since shortening of the 3'-UTR by alternative cleavage or polyadenylation was demonstrated to be involved in translational activation of oncogenes (33). RACE-PCR of the 3'-UTR resulted in a single amplicon of 135 nt, indicating that the LamB1 3'-UTR is not altered in tumorigenesis. Consistently, LamB1 northern blot analysis of two human tumor cell lines displayed single transcripts (Figure 1C). Together, these data suggest that translation of LamB1 is not regulated by alternative 5'-UTR species or shortening of the 3'-UTR.

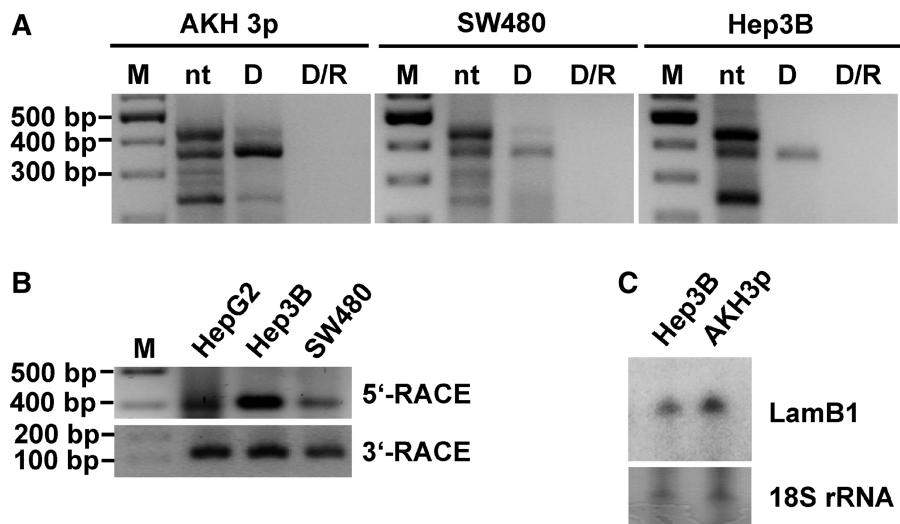


**Figure 1.** LamB1 UTRs in cancer cells. (A) The entire LamB1 5'-UTR containing 335 nt was amplified from various human cancer cells. Non-treated (nt), DNase- (D) or DNase plus RNase-treated (D/R) mRNA populations were subjected to RT-PCR (M, marker). (B) RACE-PCR of the LamB1 5'- and 3'-UTR in human cancer cell lines resulted in single amplicons of expected size. (C) Northern blot analysis revealed a single LamB1 transcript.

# Translational activation of LamB1 is IRES mediated in EMT-transformed cells

We recently showed that the LamB1 5'-UTR directs translation of a bicistronic transcript when inserted in the intercistronic region of a vector containing Renilla and Firefly luciferase reporters (19). Although this bicistronic vector is widely used there have been issues with false positive signals derived by alternative splicing (34,35). Furthermore, it has been described that intensities of IRES activities can strongly vary depending on the type of bicistronic reporters (36,37). Therefore we employed an alternative bicistronic vector encoding  $\beta$ -galactosidase ( $\beta$ -gal) as upstream and CAT as downstream reporter (34). The LamB1 5'-UTR was inserted into the intercistronic region and the empty vector served as negative control (Figure 2A). Since the cellular IRES of X linked inhibitor of apoptosis (XIAP) and its ITAFs are well documented, the minimal XIAP IRES sequence was utilized as positive control (26,38,39). Human SW480 colon carcinoma cells were transfected with bicistronic vectors and  $\beta$ -gal and CAT activities were determined (Figure 2B). Reporter activities were normalized to mRNA levels quantified by qPCR, and thus display the

ratio of active protein to bicistronic transcript levels allowing conclusions on translation efficiencies. These data show an about 7-fold increase of LamB1 IRES-mediated CAT translation as compared to control. Figure 2C normalizes CAT to cap-dependent  $\beta$ -gal translation rates of the bicistronic transcripts, indicating a >6-fold upregulation of LamB1 IRES activity. These data corroborate our recent findings and demonstrate that the LamB1 5'-UTR mediates cap-independent translation in two independent bicistronic reporter systems (19).

We next analyzed whether the IRES activity of LamB1 is regulated upon hepatocellular EMT by employing bicistronic experiments in immortalized MIM-1-4 hepatocytes, malignant epithelial MIM-R hepatocytes that were transformed with oncogenic Ras as well as in those that have undergone EMT upon TGF- $\beta$  treatment (MIM-RT). All cells were transfected with bicistronic constructs containing either the LamB1 5'-UTR, the minimal XIAP IRES or the empty vector.  $\beta$ -gal (Figure 2D) or CAT activities (Figure 2E) were normalized to transcript levels and displayed as the ratio of IRES- to cap-dependent translation (Figure 2F). As expected,  $\beta$ -gal levels displayed no significant variations of cap-dependent translation rates in the cell lines (Figure 2D). CAT activities were

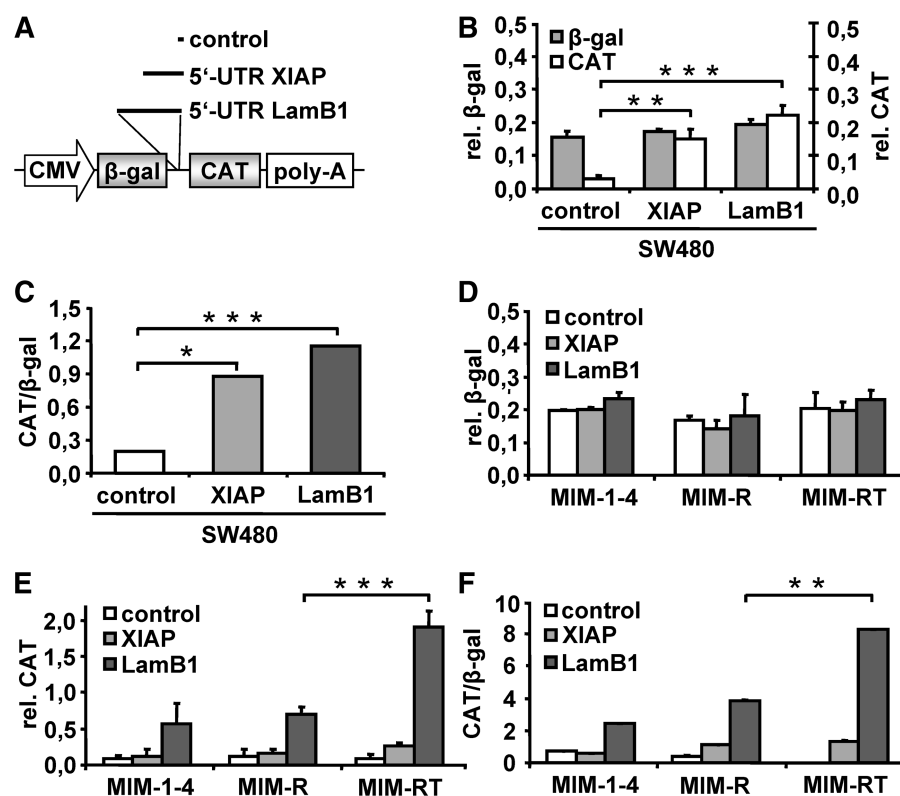


**Figure 2.** The LamB1 5'-UTR shows IRES activity that is activated during EMT. (A) Vectors employed for the bicistronic assay contain the full length LamB1 5'-UTR or the minimal XIAP IRES within the linker region of the  $\beta$ -gal and CAT reporter. The empty vector is taken as negative control. (B) SW480 colon carcinoma cells were transfected with bicistronic vector and  $\beta$ -gal and CAT activities were determined after 48 h.  $\beta$ -gal and CAT activities were normalized to transcript levels as quantified by qPCR. (C) The LamB1 5'-UTR as well as the XIAP display IRES activity in human SW480 cells. Shown is the ratio of IRES-mediated CAT to cap-dependent  $\beta$ -gal translation. (D)  $\beta$ -gal and (E) CAT activities of MIM-1-4, MIM-R and MIM-RT cells each transfected with bicistronic vectors. Cells were lysed after 48 h and reporter activities were normalized to mRNA levels as quantified by qPCR. (F) As depicted by the ratio of CAT to  $\beta$ -gal activity, MIM-RT cells that have undergone EMT by TGF- $\beta$  show significant upregulation of LamB1 IRES activity as compared to Ras-transformed malignant MIM-R hepatocytes. \* $P$  < 0.05, \*\* $P$  < 0.01 or \*\*\* $P$  < 0.005.

2.7-fold elevated in EMT-transformed MIM-RT hepatocytes as compared to epithelial MIM-R cells (Figure 2E), suggesting activation of LamB1 IRES translation upon hepatocellular EMT. Normalization of  $\beta$ -gal to CAT activities as shown in Figure 2F revealed comparable data as depicted in Figure 2E. These results are consistent with recently published data that were obtained using Renilla and Firefly luciferase reporters (19). Notably, LamB1 IRES translation showed higher levels than XIAP in the malignant progression of hepatocytes (Figure 2E and F). This effect might be cell type specific since LamB1 and XIAP exhibited similar activities in SW480 colon cancer cells (Figure 2C). Together, these data show that the LamB1 5'-UTR confers translation of the downstream cistron in the  $\beta$ -gal/CAT constructs, indicating IRES-mediated translation. Furthermore, LamB1-driven IRES translation in this assay is activated upon hepatocellular EMT which corroborates recent data (19).

### The LamB1 5'-UTR does not direct aberrant transcription or cryptic splicing

Bicistronic assays to determine IRES activity have been criticized since reporter activity of the downstream cistron may arise from the presence of cryptic promoter or splice sites within the 5'-UTR rather than from the IRES.

In order to detect any aberrant bicistronic transcripts, we performed northern blot analysis of SW480 and MIM-R cells transfected with the bicistronic vector containing LamB1 5'-UTR or empty control. Probes for the  $\beta$ -gal and CAT reporter hybridized to the bicistronic mRNA revealed single transcripts of equal size (Figure 3A). Truncated mRNAs generated from cryptic promoter or splice sites could not be detected. As northern blot analysis could fail to detect smaller transcripts due to limited sensitivity, we determined the ratio of CAT to  $\beta$ -gal cistrons by qPCR. This analysis revealed that ratios were comparable between bicistronic vectors containing either XIAP IRES, LamB1 5'-UTR or empty control (Figure 3B). These data indicate that the LamB1 5'-UTR does not direct aberrant transcription or splicing.

To further analyze cryptic promoter activity, we constructed vectors containing the LamB1 5'-UTR, the EMCV IRES or the empty control upstream of a Firefly luciferase reporter, each in presence or absence of a CMV promoter. These vectors were transfected into MIM-R hepatocytes together with a  $\beta$ -gal reporter plasmid and Firefly activities were normalized to  $\beta$ -gal levels (Figure 3C). Interestingly, promoterless plasmids showed residual luciferase activities of 6–8%. However, these remaining activities are considered to be independent of the

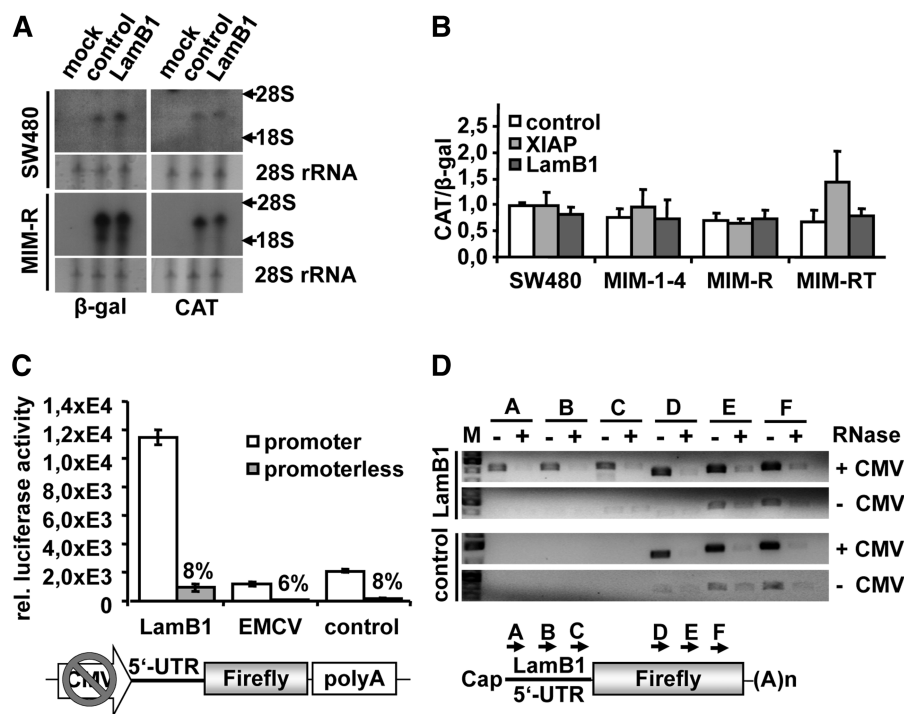


**Figure 3.** LamB1 IRES activity is not affected by cryptic promoter or splice sites. (A) Northern blot analysis of murine MIM-R hepatocytes and human SW480 colon cancer cells transfected with bicistronic constructs. Hybridization with probes for the  $\beta$ -gal and CAT reporter revealed single transcripts of equal size. Arrows indicate the position of 28S and 18S rRNA on the blot. 28S rRNA is shown as a loading control. (B) qPCR for  $\beta$ -gal and CAT in cells transfected with bicistronic vectors were normalized to RhoA levels, resulting in equal CAT to  $\beta$ -gal ratios for the vector containing LamB1 5'-UTR and empty control. (C) To test cryptic promoter activity in the LamB1 5'-UTR, the sequence was cloned upstream of a Firefly luciferase reporter and the CMV promoter was removed. The viral EMCV IRES and the empty vector were used as negative controls. Vectors were co-transfected with a  $\beta$ -gal expressing plasmid into MIM-R cells. Firefly luciferase activities were measured after 48 h and normalized to  $\beta$ -gal activities. (D) The cryptic promoter activity of the Firefly reporter was analyzed by linear semiquantitative RT-PCR using primer localized within the LamB1 5'-UTR (A–C) or the Firefly luciferase ORF (D–F). Arrows mark the position of forward primer each giving rise to an amplicon with 400–500 nt. Samples were treated with RNase to detect DNA contaminations.

sequence upstream of the luciferase reporter, since they were almost equally detected in vectors under investigation. These results suggest that cryptic transcription occurs within the Firefly luciferase, which has already been reported (40). To identify the origin of the aberrant transcription, we performed RT-PCR using primer that bind within the LamB1 5'-UTR (A-C) or within the Firefly luciferase ORF (D-F; Figure 3D). To exclude DNA contaminations RNA extracts were treated with RNase resulting in no amplicon. Only primer located within the Firefly luciferase (E,F) amplified transcripts of promoterless vectors in presence or absence of the LamB1 5'-UTR, suggesting a cryptic promoter activity within the Firefly luciferase rather than in the LamB1 5'-UTR. These data provide strong evidence that the LamB1 5'-UTR does not drive aberrant transcription and that translation of the bicistronic vector containing the LamB1 5'-UTR was indeed mediated by an IRES.

#### Determination of the minimal LamB1 IRES motif

To determine the minimal *cis*-acting IRES motif of the LamB1 5'-UTR, we generated bicistronic constructs containing deleted fragments of the 5'-UTR (Figure 4). The sequence was truncated in steps of 50 nt starting from the 5'- or 3'-end. MIM-R and MIM-RT hepatocytes were transfected with the constructs and CAT activities were normalized to  $\beta$ -gal levels. The segment between -293 and -1 upstream of the start codon retained full IRES activity, while the region between -241 and -1 showed reduced IRES activity indicating that the minimal IRES motif starts within -293 and -241. A sequence upstream of the start codon containing 82 nt (-82 to -1) displayed 31% activity of the full length 5'-UTR and therefore might have still some ability to attract the translation initiation complex. Deletion of this region caused a reduced activity

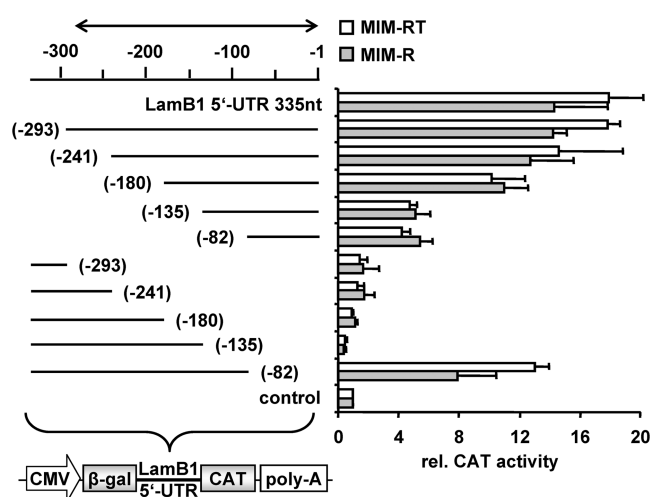


**Figure 4.** *Cis*-acting sequence requirements for LamB1 IRES activity. The sequence of the LamB1 5'-UTR was deleted in steps of approximately 50 nt starting from the 5'-UTR or 3'-UTR and cloned into the bicistronic  $\beta$ -gal/CAT reporter vector. IRES activities of bicistronic vectors were determined after transfection into MIM-R and MIM-RT cells. Lysates were analyzed after 48 h post-transfection and CAT activities were normalized to  $\beta$ -gal activities.

of the remaining fragment (-335 to -82) to 64% of the full length 5'-UTR, suggesting that it is not essential for internal ribosome binding but may work as an enhancer of IRES activity. Furthermore, a motif that regulates IRES activity in response to TGF- $\beta$  induced EMT might start within -241 to -180, since the -241 to -1 fragment is still regulated between MIM-R and MIM-RT cells while 5'-deletion to -180 nt results in similar IRES activities in both cell lines. Taken together these data reveal a minimal IRES motif required for translational activity that starts between -293 and -241 and ends between -82 and -1, and in addition, suggest an IRES domain between -241 and -180 that responds to TGF- $\beta$ .

#### La interacts with the LamB1 5'-UTR *in vitro* and *in vivo*

IRES-driven translation has been shown to be regulated by ITAFs (24). Therefore, we aimed to identify RNA-binding proteins that interact with the LamB1 5'-UTR by streptavidin-tethered RNA affinity purification. Constructs containing the LamB1 5'-UTR or the minimal XIAP IRES downstream of two S1 aptamers were generated. The minimal XIAP IRES was applied as control for selectivity since several interacting ITAFs have already been described (38,39,41). The constructs were *in vitro* transcribed and RNA was conjugated to magnetic streptavidin beads. Whole protein extracts of HEK293 cells were incubated with either streptavidin beads alone, streptavidin beads conjugated to the transcript of the LamB1 5'-UTR or streptavidin beads conjugated to the XIAP transcript. Elution with biotin allowed a high selectivity for RNA associated proteins. Analysis by SDS electrophoresis followed by silver staining revealed a 47-kDa protein that interacts with the LamB1 5'-UTR (Figure 5A). This protein was identified as La/SSB by western blot analysis (Figure 5B). The La protein as well as the 37-kDa protein hnRNP A1 bound to the XIAP control RNA. Both ITAFs have been described as regulators of XIAP IRES activity and therefore demonstrate the selectivity of this experimental approach (38,39). The control reaction using streptavidin beads alone did not yield any proteins (Figure 5A and B). From these data we concluded that La selectively binds the LamB1 5'-UTR *in vitro*.

This interaction was verified *in vivo* by anti-La RNA immunoprecipitation (IP) (Figure 5C). Lysates were generated from SW480 or HEK293 cells after UV crosslinking of RNA-protein complexes. Cell lysates were immunoprecipitated with magnetic beads conjugated to La antibody or unconjugated beads as control. RNA was isolated from either cell lysates (Input), IP with anti-La conjugated beads (La) or unconjugated beads (beads) and RT-PCR was performed. To exclude the presence of DNA contaminations, a control reaction without reverse transcription (r.t.) was included. The ability of the antibody to precipitate the La protein was verified by western blot (Supplementary Figure S1). As shown in Figure 5C, LamB1 and XIAP but not Actin transcripts could be amplified from the immunoprecipitated mRNA in both cell lines. While XIAP serves as a positive control, actin mRNA is known to lack interaction with La, showing the



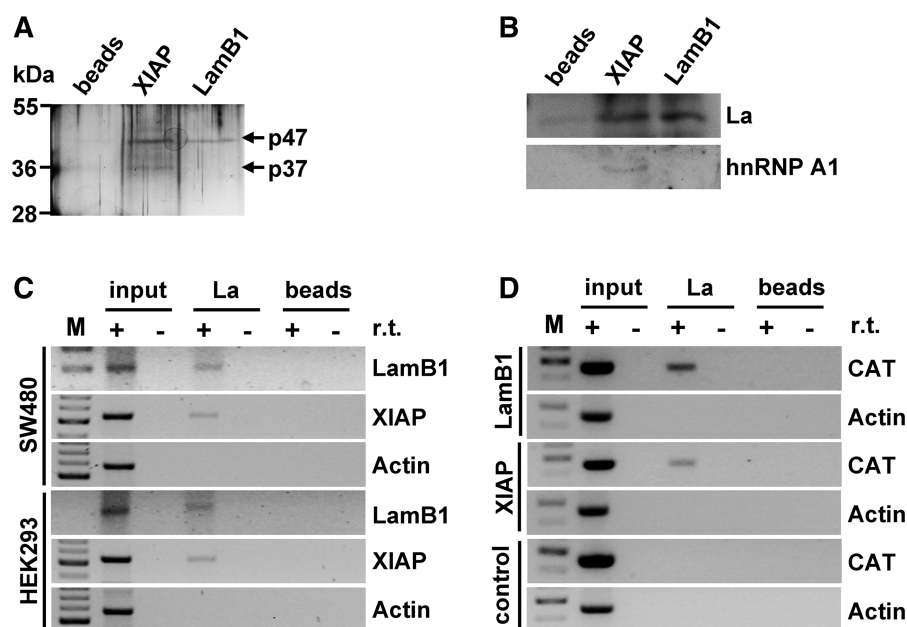


**Figure 5.** Identification of La interacting with the LamB1 IRES. (A) The LamB1 5'-UTR or XIAP minimal IRES were cloned into the pTrap vector. *In vitro* transcription of the linearized vector resulted in transcripts containing two S1 aptamers that bind streptavidin followed by the sequence of interest. The transcripts were linked to streptavidin beads and employed to pull down proteins from HEK293 cell extract. RNA-protein complexes were subjected to SDS electrophoresis. Silver staining shows a 47-kDa protein interacting with both the LamB1 and XIAP IRES and a 37-kDa protein interacting with the XIAP IRES only. (B) Proteins were identified by western blotting as La (47 kDa) and hnRNP A1 (37 kDa). (C) Lysates of UV crosslinked SW480 and HEK293 cells were subjected to RNA-IP using the La antibody followed by RT-PCR for LamB1. cDNA was generated with or without reverse transcriptase (r.t.) to detect DNA contaminations. (D) HEK293 cells were transfected with bicistronic vectors, UV crosslinked after 48 h and subjected to RNA-IP employing the La antibody followed by RT-PCR for CAT.

selectivity of the IP (42). Thus, these data indicate the physical interaction of La with the LamB1 mRNA in two different human cell lines. To further investigate this interaction and analyze whether La binds the LamB1 5'-UTR *in vivo*, the La-IP was performed in HEK293 cells transfected with the bicistronic construct containing either the LamB1 5'-UTR, the XIAP IRES or the empty control. RT-PCR for the CAT reporter revealed that La selectively binds the LamB1 5'-UTR and XIAP IRES but not the empty vector (Figure 5D). Taken together, these data show that La associates with the LamB1 5'-UTR *in vitro* and *in vivo*.

#### La binding to the LamB1 IRES is regulated upon EMT

Since La represents an ITAF that binds to the LamB1 5'-UTR, we next investigated whether the interaction between La and the LamB1 IRES is regulated during EMT. Therefore we performed La RNA-IP employing epithelial MIM-R and fibroblastoid MIM-RT hepatocytes. Cells were transfected with bicistronic vectors containing the minimal LamB1 IRES, the XIAP IRES or the empty control. RT-PCR for the CAT reporter revealed that La binds to the LamB1 and XIAP IRES in MIM-R as well as MIM-RT cells (Figure 6A). qPCR for the CAT reporter was performed to reliably quantify the amount of LamB1 bicistronic transcripts that interact with La in each cell line (Figure 6B). Quantified levels of immunoprecipitated bicistronic transcripts were normalized to the amount of bicistronic transcript that was used for the IP. Interestingly, higher levels of La protein associated

with the minimal LamB1 IRES in MIM-RT cells than in MIM-R cells suggesting that the interaction of La with the LamB1 5'-UTR is upregulated after EMT. This observation is consistent with the bicistronic assay that revealed a significant increase of IRES activity upon EMT (Figure 2F) and with recent data showing that La is an activator of several cellular IRESs (39,43,44). We further investigated the regulation of La during EMT in our cell model. Western blot analysis revealed comparable levels of La protein in MIM-R and MIM-RT cells, while LamB1 expression was clearly elevated in EMT-transformed cells (Figure 6C). Thus, La is not regulated during EMT at the level of total protein expression. As recent reports described that La can shuttle between nucleus and cytoplasm, we studied this possible mode of regulation by subcellular fractionation. Interestingly, western blot analysis showed that MIM-RT cells display increased cytoplasmic La levels compared to MIM-R cells (Figure 6D). In addition, treatment of MIM-R cells with TGF- $\beta$  resulted in slightly enhanced cytoplasmic levels of La protein. Notably, elevated levels of cytoplasmic La correlated with LamB1 upregulation. In summary, these data suggest that La protein accumulates in the cytoplasm during TGF- $\beta$  induced EMT, where it binds to the minimal LamB1 IRES motif to increase translation.

#### LamB1 IRES activity is enhanced by La

As the interaction of La with the LamB1 IRES is regulated upon EMT, we investigated whether La enhances IRES-mediated translation of LamB1.



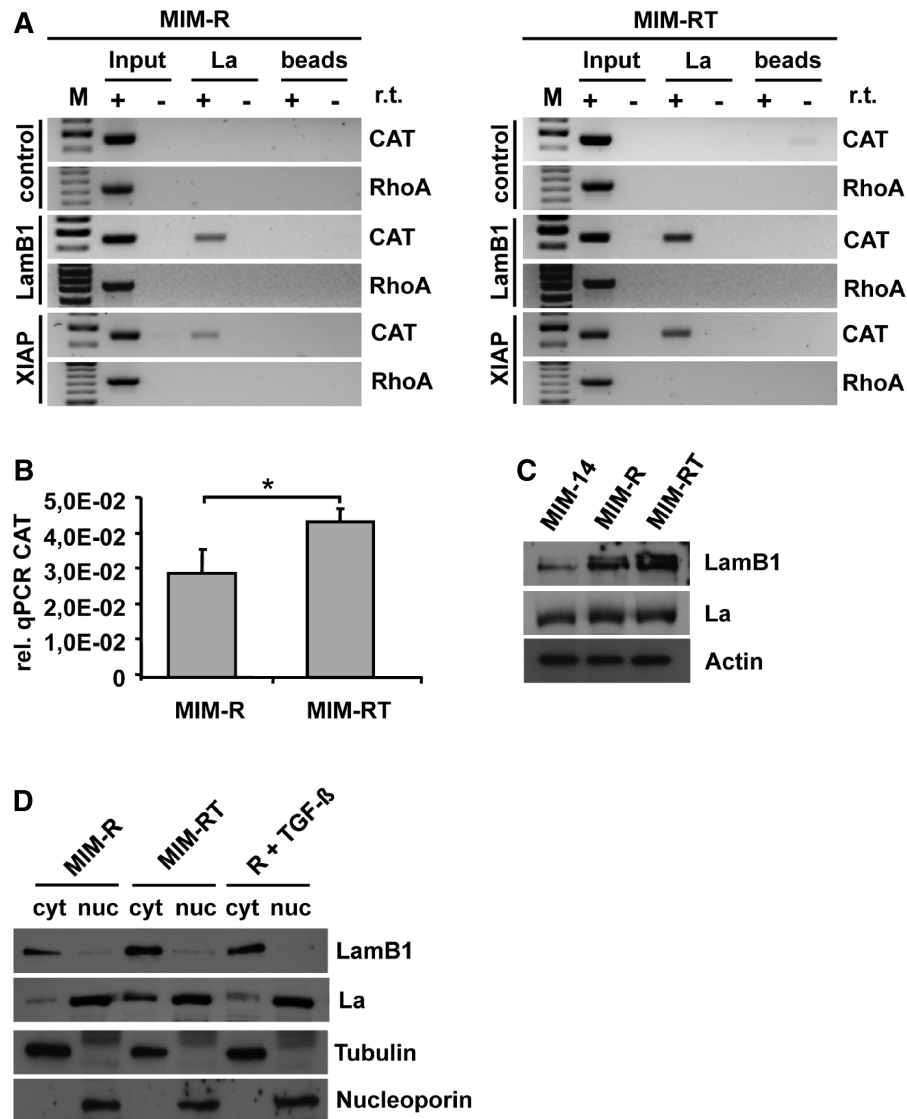


**Figure 6.** The binding of La to the LamB1 IRES is regulated upon EMT. (A) MIM-R and MIM-RT cells were transfected with bicistronic vectors containing the minimal LamB1 IRES, the minimal XIAP IRES or the empty control and after 48 h UV crosslinked prior to cell lysis. Cell extracts were immunoprecipitated with La antibody followed by RT-PCR for the CAT reporter. cDNA was generated with or without reverse transcriptase (r.t.) to detect DNA contaminations. (B) Levels of La bound to LamB1 bicistronic transcripts were quantified by qPCR and normalized to LamB1 RNA input levels. (C) Total protein levels of La and LamB1 in MIM-14, MIM-Ras and MIM-RT cells were analyzed by western blotting. (D) Nuclear and cytoplasmic fractions of MIM-R and MIM-RT cells as well as MIM-R hepatocytes treated for 24 h with 2.5 ng/ml TGF-β analyzed by western blotting. The purity of cytoplasmic and nuclear cell fractions was assessed by tubulin and nucleoporin, respectively.

Therefore, we studied the effect of La on LamB1 IRES activity using an *in vitro* translation assay (Figure 7A). Rabbit reticulocyte lysate (RRL) was programmed with *in vitro* transcribed bicistronic RNA containing the LamB1 5'-UTR and the IRES-dependent CAT activities were determined. Prior to *in vitro* translation, RRL was pre-cleared from La with magnetic beads conjugated to La antibody or incubated with unconjugated beads as control. The pre-clearing of lysates was verified by western blot analysis (Supplementary Figure S2). Treatment with unconjugated beads resulted in a slight decrease of CAT activity suggesting that some factors required for LamB1 IRES translation unspecifically bind to the beads. When RRL was pre-cleared from La, the

CAT activity was further significantly decreased (Figure 7A). Notably, the reduced LamB1 5'-UTR mediated translation could be restored by addition of recombinant La. These results suggest that La positively affects IRES-driven translation of LamB1. Since La has been described as activator of XIAP IRES translation, we employed the minimal XIAP IRES in the same experimental setting, which led to similar results [Supplementary Figure S3; (39)]. These data suggest that La works as an ITAF that binds to the minimal LamB1 IRES and enhances its translational activity during hepatocellular EMT.

To study the effect of La on LamB1 IRES translation *in vivo*, we generated MIM-R and MIM-RT cells with a

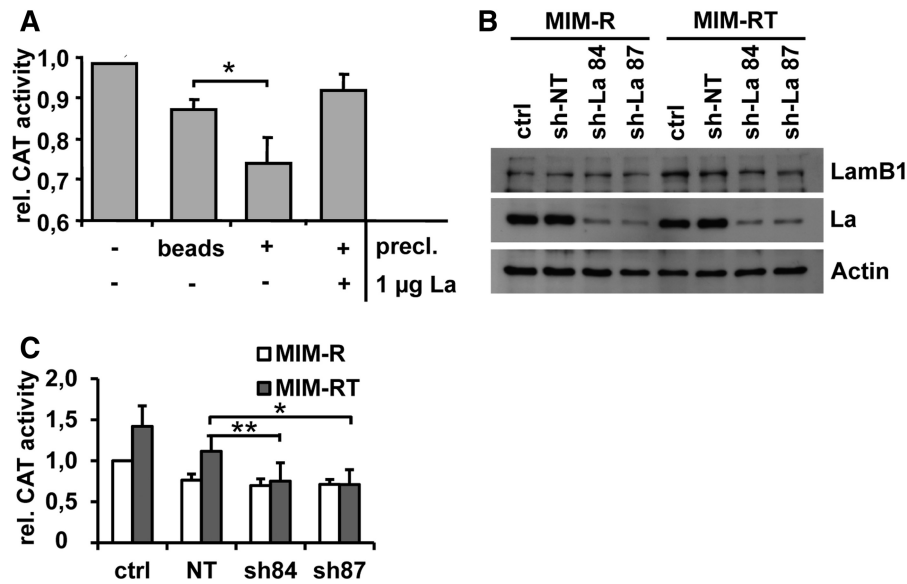


**Figure 7.** La stimulates IRES-driven Lamb1 translation. (A) Rabbit reticulocyte lysate (RRL) was programmed with the bicistronic vector containing the Lamb1 5'-UTR. Lysates were pre-cleared (precl.) with beads crosslinked to La antibody (+) or with non-conjugated beads (beads). Depletion of La from lysates reduced Lamb1 IRES-mediated translation of the CAT reporter and addition of 1  $\mu$ g recombinant La restored Lamb1 IRES activity.  $*P < 0.05$ . (B) MIM-R and MIM-RT cells were lentivirally infected with two different shRNA constructs against La (shLa 84, shLa 87) or non-target shRNA (sh-NT). The knock-down of La compared to the untreated control (ctrl) as detected by western blotting. (C) The generated cell lines were transfected with a bicistronic vector containing the Lamb1 5'-UTR. Lysates were analyzed 48 h post-transfection and CAT activities were normalized to  $\beta$ -gal activities.  $*P < 0.05$  or  $**P < 0.01$ .

stable knock-down of La expression. Western blot analysis revealed a strong knock-down of La using two different shRNA constructs (shLa 84, shLa 87) as compared to non-target control (sh-NT) or untreated cells (ctrl) (Figure 7B). Notably, MIM-RT but not MIM-R cells showed reduced levels of Lamb1 after knock-down of La. These data suggest that La mediated stimulation of IRES-driven Lamb1 translation after EMT is diminished by silencing of La. To further study the effect of impaired La expression on Lamb1 IRES activity, bicistronic assays were performed (Figure 7C). MIM-R and MIM-RT cells with a stable knock-down of La (shLa 84, shLa 87), non-target shRNA (sh-NT) or the untreated control (ctrl) were transfected with a bicistronic vector containing the Lamb1 5'-UTR. Remarkably, Lamb1 IRES activity was significantly reduced in EMT-transformed MIM-RT cells harboring a La knock-down. In contrast, the knock-down of La had no significant effect on Lamb1 IRES activity in MIM-R cells. These data concurs with the regulation of Lamb1 protein expression (Figure 7B), indicating that La enhances IRES-mediated translation during EMT, which is impaired after knock-down of La.

## DISCUSSION

Lamb1 is the  $\beta$ -subunit of laminin isoforms that constitute the ECM and contribute to tumor invasion and metastasis. The control of Lamb1 expression at the transcriptional level by retinoic acid is well described, while the regulation at the level of translation is poorly understood (45). We recently provided first evidence for IRES-mediated translation of the Lamb1 5'-UTR by

using bicistronic Renilla-Firefly luciferase assays (19). However, it has been reported that the level of IRES activity can strongly vary depending on the type of bicistronic reporters (36,37). In addition, suspicious splicing has been detected with a Renilla-Firefly luciferase vector (34,35). To verify our recent results, we therefore utilized an alternative bicistronic system encoding  $\beta$ -gal as upstream and CAT as downstream reporter (34). Consistently, the Lamb1 5'-UTR was able to mediate cap-independent translation of the downstream cistron in murine and human cell lines (Figure 2). Interestingly, the bicistronic activity of Lamb1 and minimal XIAP IRES was similar in human SW480 colon cancer cells while it was strongly increased in murine MIM hepatocytes. These data indicate that the Lamb1 IRES activity depends on the cellular context rather than on the bicistronic vector used for the determination of IRES activity.

Since bicistronic activity of the downstream reporter may result from cryptic promoter or splice sites within the 5'-UTR, we performed various assays to reliably exclude aberrant transcripts. Northern blot analysis as well as qPCR for  $\beta$ -gal and CAT reporters did not reveal any truncated bicistronic mRNAs (Figure 3). Noteworthy, the accurate determination of cryptic promoter activity by employing a monocistronic Firefly luciferase vector resulted in residual reporter activities after removal of the CMV promoter (Figure 3C). These enzymatic activities were detected independently of the presence of the Lamb1 5'-UTR. RT-PCR revealed short transcripts generated by the Firefly luciferase reporter of the promoterless vector indicating a cryptic activity of the reporter itself as already described [Figure 3D, (40)].

Thus, stringent assays to detect aberrant transcripts corroborate a *bona fide* IRES activity of the LamB1 5'-UTR (19), which requires a minimal *cis*-acting IRES motif localized between -293 and -1 nt upstream of the start codon (Figure 4).

IRES-mediated *de novo* synthesis of proteins involved in angiogenesis, apoptosis or mitosis plays an important role during tumorigenesis. We initially found by expression profiling that LamB1 is translationally upregulated in Ras-transformed hepatocytes (MIM-R) that undergo EMT in response to TGF- $\beta$  (MIM-RT) (19). In this study, the bicistronic assay showed a 2.7-fold increase of IRES activity in EMT-transformed cells suggesting that elevated LamB1 levels result from activated IRES translation (Figure 2E). However, diverse mechanisms are known to account for selective translational control in cancer cells including alternative splicing of the 5'- or 3'-UTR shortening through alternative cleavage or polyadenylation (30,33). To test a possible involvement of transcript species in the regulation of LamB1 expression during tumorigenesis, we performed RACE-PCR of the 5'- and 3'-UTR. No alternative transcript variants could be detected in different human carcinoma cell lines (Figure 1B). These results are consistent with northern blot analysis suggesting that LamB1 translation is not regulated by alternative splicing or 3'-UTR shortening (Figure 1C). Therefore, the elevated translation of LamB1 upon EMT is caused by IRES activation and does not involve alternative splicing or 3'-UTR shortening.

Hence, we next aimed to identify ITAFs that interact with the LamB1 IRES and activate its translation upon EMT. Streptavidin-tethered RNA affinity purification with a transcript containing the LamB1 5'-UTR downstream of two S1 aptamers revealed that La selectively binds the 5'-UTR *in vitro* (Figure 5A). This finding was verified *in vivo* by an anti-La RNA-IP of UV crosslinked cells in two human cell lines (Figure 5C). Consistent with our data, a recently published RNA-IP of BCR/ABL-transformed myeloid cells revealed LamB1 mRNA associated to La but not to hnRNP A1, hnRNP E2 or hnRNP K (42). Furthermore, La binds the LamB1 5'-UTR as well as the minimal LamB1 IRES within the bicistronic transcript after transient transfection of cells (Figures 5D and 6A). The amount of La that is associated with the minimal IRES is significantly elevated in EMT-transformed MIM-RT cells as compared to MIM-R hepatocytes (Figure 6B). Accordingly, western blot analysis of cytoplasmic and nuclear cell fractions revealed the cytoplasmic translocation of La in response to TGF- $\beta$  induced EMT (Figure 6D). Furthermore, La enhanced LamB1 IRES activity in an *in vitro* translation assay (Figure 7A), suggesting that the elevated levels of LamB1 in EMT-transformed cells results from increased IRES-mediated translation in the presence of cytoplasmic La. In line with these data, the stable knock-down of La significantly reduced LamB1 IRES activity of a bicistronic construct in EMT-transformed cells (Figure 7C). In addition, endogenous LamB1 protein levels were decreased in La-silenced mesenchymal cells (Figure 7B). In contrast, La knock-down in epithelial cells did not

affect LamB1 IRES translation and endogenous LamB1 protein levels. In summary, these results suggest that La accumulates in the cytoplasm during hepatocellular EMT, where it binds the minimal LamB1 IRES motif to enhance IRES-mediated translation.

A role of La in the LamB1 regulation during EMT is of particular interest as recent studies suggest an important role of La in carcinogenesis. La is a RNA-binding protein involved in RNA processing and translation that predominantly localizes in the nucleus (46). Elevated La levels have been reported in chronic myeloid leukemia cells, cervical cancer and several types of cancer cell lines (19,47,48). La was shown to activate IRES-dependent translation of XIAP which supports tumorigenesis by preventing apoptosis (39). In addition, La regulates the IRES-mediated expression of cyclin D1 that stimulates cell proliferation (19). Accordingly, we found cyclin D1 translationally upregulated in MIM-RT hepatocytes that have undergone EMT by employing polysome-bound versus total RNA (data not shown). Furthermore, AKT-dependent shuttling of La to the cytoplasm leads to translational activation of a specific mRNA subset in glial cells suggesting that La could be involved in oncogenic effects of aberrant AKT activation in cancer cells (49). In this respect, it will be of relevance to dissect the molecular mechanisms of La activated LamB1 IRES translation in the context of EMT that is induced by the synergy of Ras and TGF- $\beta$  signaling and involves the activation of AKT and MAPK pathways (18).

## SUPPLEMENTARY DATA

Supplementary Data are available at NAR Online.

## ACKNOWLEDGEMENTS

The authors are grateful to Dr M. Holcik for the generous gift of pBgal/5'(-162)/CAT plasmid and Dr M. Dienstbier for the courtesy of providing the pTrap vector. Furthermore, the authors thank Dr M. Holcik and Dr M. Mokrejs for helpful advice and stimulating discussions. In particular, the authors appreciate the help of Dr M. Mokrejs to make our plasmid sequence data online available at the IRESite database (<http://iresite.org/>). This work is dedicated to Hartmut Beug who died from cancer.

## FUNDING

Funding for open access charge: Austrian Science Fund (FWF) (grant number P20905, SFB F28).

*Conflict of interest statement.* None declared.

## REFERENCES

1. Klominek, J., Robert, K. and Sundqvist, K. (1993) Chemotaxis and haptotaxis of human malignant mesothelioma cells: effects of fibronectin, laminin, type IV collagen and an autocrine motility factor-like substance. *Cancer Res.*, **53**, 4376–4382.



2. Malinda, K. and Kleinman, H. (1996) The laminins. *Int. J. Biochem. Cell Biol.*, **28**, 957–959.
3. Taniguchi, Y., Ido, H., Sanzen, N., Hayashi, M., Sato-Nishiuchi, R., Futaki, S. and Sekiguchi, K. (2009) The C-terminal Region of Laminin  $\beta$  Chains Modulates the Integrin Binding Affinities of Laminins. *J. Biol. Chem.*, **284**, 7820–7831.
4. Kim, K., Chung, J. and Kim, K. (2005) 67-kDa laminin receptor promotes internalization of cytotoxic necrotizing factor 1-expressing *Escherichia coli* K1 into human brain microvascular endothelial cells. *J. Biol. Chem.*, **280**, 1360–1368.
5. Akache, B., Grimm, B., Pandey, K., Yant, S., Xu, H. and Kay, M. (2006) The 37/67-kilodalton laminin receptor is a receptor for adeno-associated virus serotypes 8, 2, 3, and 9. *J. Virol.*, **80**, 9831–9836.
6. Massia, S., Sekhar, S. and Hubbel, J. (1993) Covalently immobilized laminin peptide Tyr-Ile-Gly-Ser-Arg (YIGSR) supports cell spreading and colocalization of the 67-kilodalton laminin receptor with  $\alpha$ -actinin and vinculin. *J. Biol. Chem.*, **268**, 8053–8059.
7. Sanjuán, X., Fernández, P., Miquel, R., Muñoz, J., Castronovo, V., Ménard, S., Palacín, A., Cardesa, A. and Campo, E. (1996) Overexpression of the 67-kD laminin receptor correlates with tumour progression in human colorectal carcinoma. *J. Pathol.*, **179**, 376–380.
8. Martignone, S., Ménard, S., Bufalino, R., Cascinelli, N., Pellegrini, R. and Tagliabue, E. (1993) Prognostic significance of the 67-kilodalton laminin receptor expression in human breast carcinomas. *J. Natl Cancer Inst.*, **85**, 398–402.
9. Tarabozetti, G., Belotti, D., Giavazzi, R., Sobel, M. and Castronovo, V. (1993) Enhancement of metastatic potential of murine and human melanoma cells by laminin receptor peptide G: attachment of cancer cells to subendothelial matrix as a pathway for hematogenous metastasis. *J. Natl Cancer Inst.*, **85**, 235–240.
10. Ueberham, E., Loew, R., Ueberham, U., Schoenig, K., Bujard, H. and Gebhardt, R. (2003) Conditional tetracycline-regulated expression of TGF- $\beta$ 1 in liver of transgenic mice leads to reversible intermediary fibrosis. *Hepatology*, **37**, 1067–1078.
11. Lim, S., Park, S., Kim, W., Park, S., Kim, H., Kim, Y., Sohn, T., Noh, J. and Jung, G. (2002) Proteome Analysis of Hepatocellular Carcinoma. *Biochem. Biophys. Res. Commun.*, **291**, 1031–1037.
12. Ozaki, I., Yamamoto, K., Mizuta, T., Kajihara, S., Fukushima, N., Setoguchi, Y., Morito, F. and Sakai, T. (1998) Differential expression of laminin receptors in human hepatocellular carcinoma. *Gut*, **43**, 837–842.
13. Begum, N., Mori, M., Matsumata, T., Takenaka, K., Sugimachi, K. and Barnard, G. (1995) Differential display and integrin  $\alpha$ 6 messenger RNA overexpression in hepatocellular carcinoma. *Hepatology*, **22**, 1447–1455.
14. Yao, M., Zhou, X., Zha, X., Shi, D., Fu, J., He, J., Lu, H. and Tang, Z. (1997) Expression of the integrin  $\alpha$ 5 subunit and its mediated cell adhesion in hepatocellular carcinoma. *J. Cancer Res. Clin. Oncol.*, **123**, 435–440.
15. Arias, A.M. (2001) Epithelial mesenchymal interactions in cancer and development. *Cell*, **105**, 425–431.
16. Bedossa, P., Peltier, E., Terris, B., Franco, D. and Poynard, T. (1995) Transforming growth factor- $\beta$ 1 (TGF- $\beta$ 1) and TGF- $\beta$ 1 receptors in normal, cirrhotic, and neoplastic human livers. *Hepatology*, **21**, 760–766.
17. Oft, M., Peli, J., Rudaz, C., Schwarz, H., Beug, H. and Reichmann, E. (1996) TGF- $\beta$ 1 and Ha-Ras collaborate in modulating the phenotypic plasticity and invasiveness of epithelial tumor cells. *Genes Dev.*, **10**, 2462–2477.
18. Gotzmann, J., Huber, H., Thallinger, C., Wolschek, M., Jansen, B., Schulte-Hermann, R., Beug, H. and Mikulits, W. (2002) Hepatocytes convert to a fibroblastoid phenotype through the cooperation of TGF- $\beta$ 1 and Ha-Ras: steps towards invasiveness. *J. Cell Sci.*, **115**, 1189–1202.
19. Petz, M., Kozina, D., Huber, H., Siwec, T., Seipelt, J., Sommergruber, W. and Mikulits, W. (2007) The leader region of Laminin B1 mRNA confers cap-independent translation. *Nucleic Acids Res.*, **35**, 2473–2482.
20. Holcik, M. (2004) Targeting translation for treatment of cancer - a novel role for IRES? *Curr. Cancer Drug Targets*, **4**, 299–311.
21. Koritzinsky, M., Magagnin, M., van den Beucken, T., Seigneuric, R., Savelkoul, K., Dostie, J., Pyronnet, S., Kaufman, R.J., Wepler, S.A., Voncken, J.W. *et al.* (2006) Gene expression during acute and prolonged hypoxia is regulated by distinct mechanisms of translational control. *EMBO J.*, **25**, 1114–1125.
22. Koromilas, A.E., Lazaris-Karatzas, A. and Sonenberg, N. (1992) mRNAs containing extensive secondary structure in their 5' non-coding region translate efficiently in cells overexpressing initiation factor eIF-4E. *EMBO J.*, **11**, 4153–4158.
23. Larsson, O.L.S., Issaenko, O., Avdulov, S., Peterson, M., Smith, K., Bitterman, P. and Polunovsky, V. (2007) Eukaryotic translation initiation factor 4E induced progression of primary human mammary epithelial cells along the cancer pathway is associated with targeted translational deregulation of oncogenic drivers and inhibitors. *Cancer Res.*, **67**, 6814–6824.
24. King, H.A., Cobbold, L.C. and Willis, A.E. (2010) The role of IRES trans-acting factors in regulating translation initiation. *Biochem. Soc. Trans.*, **38**, 1581–1586.
25. Komar, A.A. and Hatzoglou, M. (2011) Cellular IRES-mediated translation. *Cell Cycle*, **10**, 229–240.
26. Holcik, M., Lefebvre, C., Yeh, C., Chow, T. and Korneluk, R.G. (1999) A new internal-ribosome-entry-site motif potentiates XIAP-mediated cytoprotection. *Nat. Cell Biol.*, **1**, 190–192.
27. Dienstbier, M., Boehl, F., Li, X. and Bullock, S.L. (2009) Egalitarian is a selective RNA-binding protein linking mRNA localization signals to the dynein motor. *Genes Dev.*, **23**, 1546–1558.
28. Mikula, M., Fuchs, E., Huber, H., Beug, H., Schulte-Hermann, R. and Mikulits, W. (2004) Immortalized p19ARF null hepatocytes restore liver injury and generate hepatic progenitors after transplantation. *Hepatology*, **39**, 628–634.
29. Fischer, A.N., Herrera, B., Mikula, M., Proell, V., Fuchs, E., Gotzmann, J., Schulte-Hermann, R., Beug, H. and Mikulits, W. (2005) Integration of Ras subeffector signaling in TGF- $\beta$  mediated late stage hepatocarcinogenesis. *Carcinogenesis*, **26**, 931–942.
30. Xu, Q. and Lee, C. (2003) Discovery of novel splice forms and functional analysis of cancer-specific alternative splicing in human expressed sequences. *Nucleic Acids Res.*, **31**, 5635–5643.
31. Mathews, D.H., Sabina, J., Zuker, M. and Turner, D.H. (1999) Expanded sequence dependence of thermodynamic parameters improves prediction of RNA secondary structure. *J. Mol. Biol.*, **288**, 911–940.
32. Mathews, D.H., Disney, M.D., Childs, J.L., Schroeder, S.J., Zuker, M. and Turner, D.H. (2004) Incorporating chemical modification constraints into a dynamic programming algorithm for prediction of RNA secondary structure. *Proc. Natl. Acad. Sci. USA*, **101**, 7287–7292.
33. Mayr, C. and Bartel, D.P. (2009) Widespread shortening of 3'UTRs by alternative cleavage and polyadenylation activates oncogenes in cancer cells. *Cell*, **138**, 673–684.
34. Holcik, M., Graber, T., Lewis, S.M., Lefebvre, C.A., Lacasse, E. and Baird, S. (2005) Spurious splicing within the XIAP 5' UTR occurs in the *luc/Fluc* but not the *bgal/CAT* bicistronic reporter system. *RNA*, **11**, 1605–1609.
35. Van Eden, M.E., Byrd, M.P., Sherrill, K.W. and Lloyd, R.E. (2004) Demonstrating internal ribosome entry sites in eukaryotic mRNAs using stringent RNA test procedures. *RNA*, **10**, 720–730.
36. Nevins, T.A., Harder, Z.M., Korneluk, R.G. and Holcik, M. (2003) Distinct regulation of IRES-mediated translation following cellular stress is mediated by apoptotic fragments of eIF4G family members eIF4GI and p97/DAP5/NAT1. *J. Biol. Chem.*, **278**, 3572–3579.
37. Jopling, C.L., Belsham, G.J. and Willis, A.E. (2000) Analysis of the c-myc IRES: a potential role for cell-type specific trans-acting factors and the nuclear compartment. *Nucleic Acids Res.*, **28**, 687–694.
38. Lewis, S.M., Veyrier, A., Ungureanu, N.H., Bonnal, S., Vagner, S. and Holcik, M. (2007) Subcellular relocalization of a trans-acting factor regulates XIAP IRES-dependent translation. *Mol. Biol. Cell*, **18**, 1302–1311.
39. Holcik, M. and Korneluk, R.G. (2000) Functional characterization of the X-linked inhibitor of apoptosis (XIAP) internal ribosome entry site element: role of La autoantigen in XIAP translation. *Mol. Cell Biol.*, **20**, 4648–4657.

40. Vopalensky,V., Masek,T., Horvath,O., Vicensova,B., Mokrejs,M. and Pospisek,M. (2008) Firefly luciferase gene contains a cryptic promoter. *RNA*, **14**, 1720–1729.
41. Holcik,M., Gordon,B.W. and Korneluk,R.G. (2003) The internal ribosome entry site-mediated translation of antiapoptotic protein XIAP is modulated by the heterogeneous nuclear ribonucleoproteins C1 and C2. *Mol. Cell. Biol.*, **23**, 280–288.
42. Eiring,A.M., Neviani,P., Santhanam,R., Oaks,J.J., Chang,J.S., Notari,M., Willis,W., Gambacorti-Passerini,C., Volinia,S., Marcucci,G. *et al.* (2008) Identification of novel posttranscriptional targets of the BCR/ABL oncoprotein by ribonomics: requirement of E2F3 for BCR/ABL leukemogenesis. *Blood*, **111**, 816–828.
43. Kim,J.K., Back,S.H., Rho,J., Lee,S.H. and Jang,S.K. (2001) La autoantigen enhances translation of BIP mRNA. *Nucleic Acids Res.*, **29**, 5009–5016.
44. Sommer,G., Dittmann,J., Kuehnert,J., Reumann,K., Schwartz,P.E., Will,H., Coulter,B.L., Smith,M.T. and Heise,T. (2011) The RNA-binding protein La contributes to cell proliferation and CCND1 expression. *Oncogene*, **30**, 434–444.
45. Li,C. and Gudas,L.J. (1996) Murine laminin B1 gene regulation during the retinoic acid- and dibutyryl cyclic AMP-induced differentiation of embryonic F9 teratocarcinoma stem cells. *J. Biol. Chem.*, **271**, 6810–6818.
46. Wolin,S.L. and Cedervall,T. (2002) The La protein. *Annu. Rev. Biochem.*, **71**, 375–403.
47. Trotta,R., Vignudelli,T., Candini,O., Intine,R.V., Pecorari,L. and Guerzoni,C. (2003) BCR/ABL activates mdm2 mRNA translation via the La antigen. *Cancer Cell*, **3**, 145–160.
48. Al-Ejeh,F., Darby,J.M. and Brown,M.P. (2007) The La autoantigen is a malignancy-associated cell death target that is induced by DNAdamaging drugs. *Clin Cancer Res.*, **13**, 5509–5518.
49. Brenet,F., Socci,N.D., Sonenberg,N. and Holland,E.C. (2009) Akt phosphorylation of La regulates specific mRNA translation in glial progenitors. *Oncogene*, **28**, 128–139.